Automated Defect Inspection Systems by Pattern Recognition

Mira Park[1], Jesse S. Jin[1], Sherlock L. Au[2], Suhuai Luo[1], and Yue Cui[1]
[1]*The School of Design, Communication & IT, The University of Newcastle, Australia*
[2]*Multi Base Ltd, Hong Kong*
mira.park@newcastle.edu.au

Abstract

Visual inspection and classification of cigarettes packaged in a tin container is very important in manufacturing cigarette products that require high quality package presentation. For accurate automated inspection and classification, computer vision has been deployed widely in manufacturing. We present the detection of the defective packaging of tins of cigarettes by identifying individual objects in the cigarette tins. Object identification information is used for the classification of the acceptable cases (correctly packaged tins) or defective cases (incorrectly packaged tins). This paper investigates the problem of identifying the individual cigarettes and a paper spoon in the packaged tin using image processing and morphology operations. The segmentation performance was evaluated on 500 images including examples of both good cases and defective cases.

Keywords: *Pattern Recognition, Automated Defect Inspection Systems, Cigarette*

1. Introduction

Package inspection systems are continuously conveyed in the manufacturing process. The systems are capable of measuring predetermined parameters of packages, comparing the measured parameters with predetermined values, evaluating from the measured parameters the integrity of the packages and determining whether such packages are acceptable or, alternatively, whether they should be rejected.

Humans are able to find such defects with prior knowledge. Human judgment is influenced by expectations and prior knowledge. However, it is tedious, laborious, costly and inherently unreliable due to its subjective nature. Therefore, traditional visual quality inspection performed by human inspectors has the potential to be replaced by computer vision systems[1-7]. The increased demands for objectivity, consistency and efficiency have necessitated the introduction of accurate automated inspection systems. These systems employ image processing techniques and can quantitatively characterize complex sizes, shapes, and the color and textural properties of products.

Accurate automated inspection and classification can reduce human workloads and labor costs while increasing the throughput. A large amount of research has been carried out on automated inspection of tile surfaces [8-13], biscuit bake color [14], the color of potato chips [15], textile fabrics [16-23], food products [24-26] [27] and wood [28, 29]. However, relatively little work has been done in automated defect classification, mainly because of the difficult nature of the problem. Computer vision has been used to objectively measure the color of different food since it provides some additional and obvious advantages over a conventional techniques such as using a colorimeter, namely, the possibility of analyzing each pixel of the entire surface of the food, and quantifying the surface characteristics and defects [30] [31].

Table 1. The examples of the good cases and the defective cases

GOOD CASES	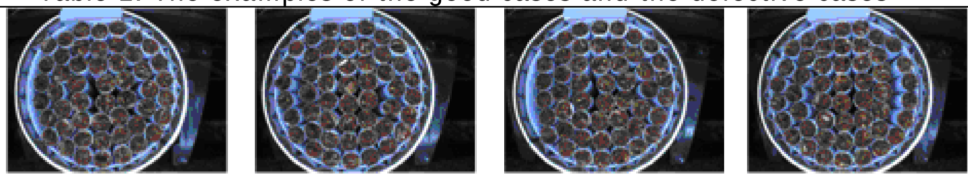
DEFECTIVE CASES	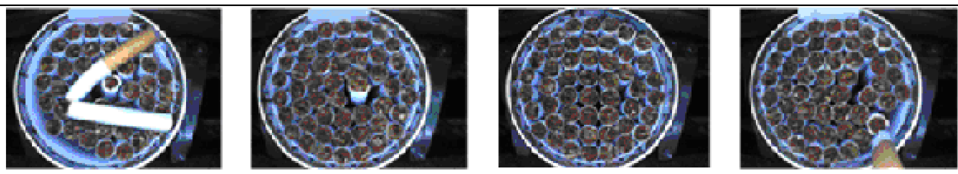

The most difficult problem is the segmentation of the background and the foreground and the extraction of the important information in the foreground. The segmentation process partitions the digital image into disjoint regions. Segmentation is an essential step in computer vision and automatic pattern recognition processes that are based on an image analysis of foregrounds, as subsequent extracted data are highly dependent on the accuracy of this initial operation. In general, automated segmentation is one of the most difficult tasks in the image analysis process, because a false segmentation will cause degradation of the measurement process and therefore the interpretation may fail.

Visual inspection and classification of cigarette tin packages are very important in the manufacturing of cigarette products that require high quality packaging and presentation. For accurate automated inspection and classification, computer vision has been deployed widely in the manufacturing process. For example Yeh[14] used Kohonen's selforganising map for identifying baking curves of baked goods, Zhang and Bresee [32] detected defective images in textile fabrics by individually applying simple classification to discriminate knots from slubs according to the ratio of length to width, and Brazakovic [28] employed a pyramid-linking scheme to locate defects in wood and a hierarchical defect classification scheme to classify four types of wood defect.

Computer vision is a novel technology for acquiring and analyzing an image of a real scene by computers and other devices in order to obtain information, or to control processes. The core technique in computer vision is always related to image processing, which can lead to segmentation, qualification and then classification of images and objects of interest within images.

In this paper, we present the segmentation of the foreground objects and the identification of the individual objects in a cigarette tin package, where this information will be used for the classification of packaging into either acceptable or defective cases [see Table1].

2. Methods

2.1. Counting objects in an image

2.1.1. Color-Based Segmentation of the Region of Interests

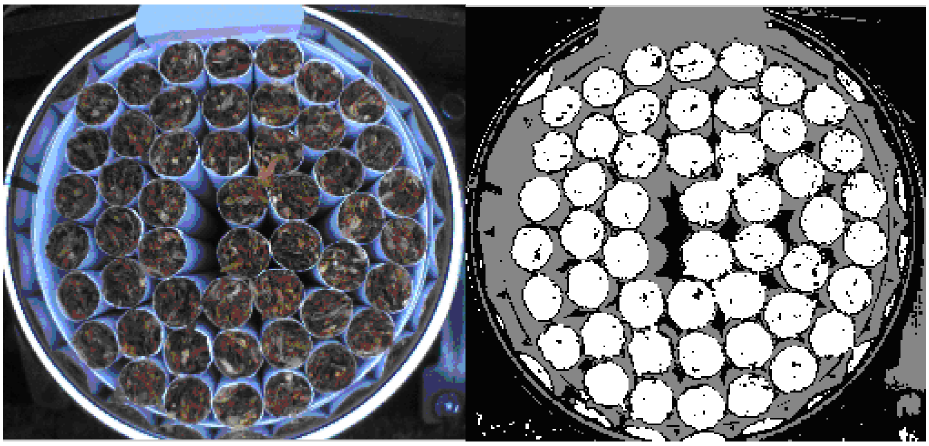

Figure 1. Input image (left) and Image labelled by cluster index (right)

We use the $L^*a^*b^*$ color space to segment colors in an automated fashion. The $L^*a^*b^*$ color space is a color-opponent with dimension L^* for Lightness and a^* and b^* for the color-opponent dimensions, based on nonlinearly-compressed CIE XYZ color space coordinates [33][34].

Step 1: Convert image from RGB color space to L*a*b* color space.

Color is a determining factor in the identifying of the objects in an image. With a digital camera it is possible to register the color of any pixel of the image of the object using three color sensors per pixel [35]. The most often used color model is the RGB model in which each sensor captures the intensity of the light in the red(R), green(G) or blue(B) spectrum, respectively. The human vision system developed a way to correct for the quality of illumination, and to preserve differences in hue. A white paper is perceived as white even in reddish evening light. To allow similar possibilities is in color measurement, CIE (Commission on Internationale de l'Eclairage) defined several more human-related, less illumination-dependent measures of color, of which the most common is $L^*a^*b^*$ [36].

There are mainly three colors in our input image if we ignore variations in brightness: white, black, brown. The $L^*a^*b^*$ color space enables to quantify these visual differences since the $L^*a^*b^*$ color is designed to approximate human vision. It aspires to perceptual uniformity, and its L^* component closely matches human perception of lightness. It can thus be used to make accurate color balance corrections by modifying output curves in the a^* and b^* components, or to adjust the lightness contrast using the L^* component. The L*a*b* space consists of a luminosity layer L^*, the chromaticity-layer a^* indicating where color falls along the red-green axis, and the chromaticity-layer b^* indicating where the color falls along the blue-yellow axis.

The methodology used for estimating the RGB → $L^*a^*b^*$ transformation consists of two parts [37].

(i) Definition of the model: The model has parameters θ_1, θ_2, … θ_m whose inputs are the RGB variables obtained from the color digital image of a sample, and whose outputs are the $L^*a^*b^*$ variables estimated from the model; and

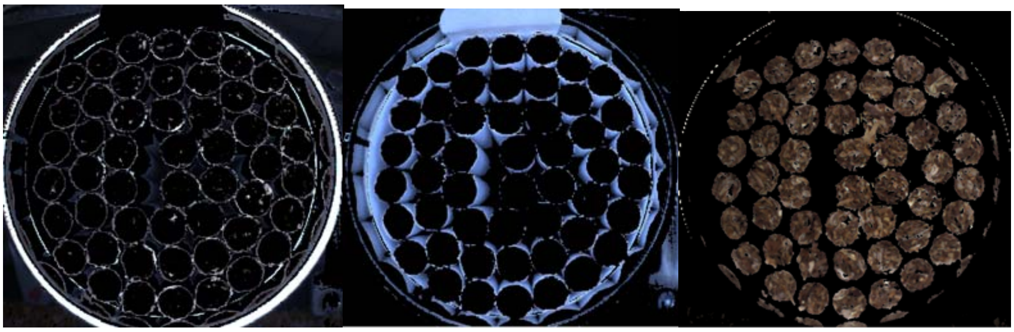

Figure 2. Separated objects by colour. left: objects in cluster 1, middle: objects in cluster 2, right: objects in cluster 3

(ii) Calibration: The parameters θ_1, θ_2, … ,θ_m for the model are estimated on the basis of the minimization of the mean absolute error between the estimated variables (model output) $\hat{L}^*, \hat{a}^*, \hat{b}^*$ and the L^*, a^*, b^* variables that are measured from the sample used in (i) through the use of a colorimeter.

Construction of Linear Model

In this, the simplest model of all, the RGB → L*a*b* transformation is a linear function of the (R, G, B) variables:

$$\begin{bmatrix} \hat{L}^* \\ \hat{a}^* \\ \hat{b}^* \end{bmatrix} = \begin{bmatrix} M_{11} & M_{12} & M_{13} & M_{14} \\ M_{21} & M_{22} & M_{23} & M_{24} \\ M_{31} & M_{32} & M_{33} & M_{34} \end{bmatrix} \begin{bmatrix} R \\ G \\ B \\ I \end{bmatrix}$$

The following is an explanation of how the parameters of the first row of matrix **M** are obtained (the same explanation is valid for the other rows): We first must define the parameters vector for the model

$$\theta = \begin{bmatrix} M_{11} & M_{12} & M_{13} & M_{14} \end{bmatrix}^T$$

The input matrix with N measurements of R, G, B

$$X = \begin{bmatrix} R_1 & G_1 & B_1 & 1 \\ \vdots & \vdots & \vdots & \vdots \\ R_N & G_N & B_N & 1 \end{bmatrix}$$

And the output vector with the N measurements of L^*

$$y = \begin{bmatrix} L_1^* & \dots & L_N^* \end{bmatrix}^T$$

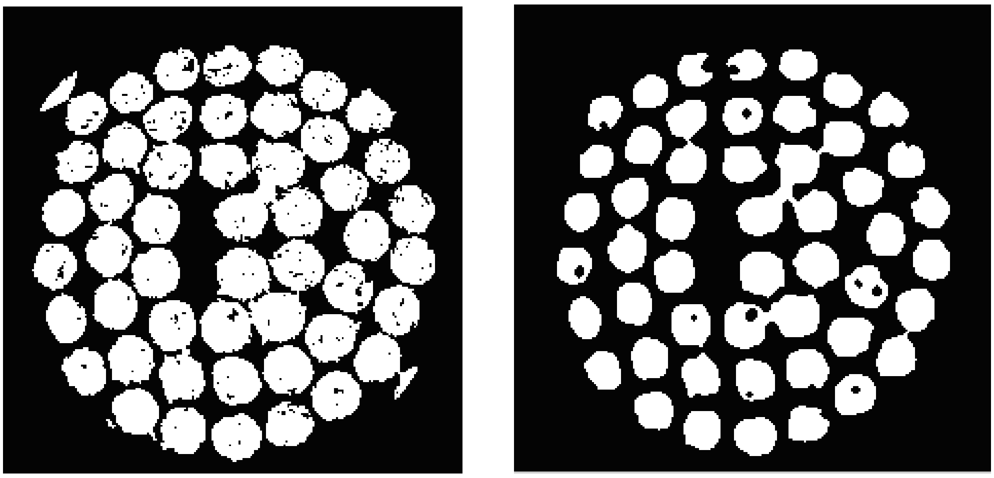

Figure 3. The left image is the binary image of the segmented image and the right image is the simplified image of the left image

thus the estimate of L^*, obtained from the minimization of the norm between measurements and estimated $\left\| y - \hat{y} \right\|$, is defined by [38]:

$$\hat{y} = X\theta$$

where

$$\theta = \left[X^T X\right]^{-1} X^T y$$

The advantage of this model is that it is direct and its solution is not obtained through iterations.

Step2: Classify the colors in ‘a*b*’ space using K-means clustering

We use K-means clustering to separate groups of objects. K-means clustering treats each object as having a location in space. It finds partitions such that objects within each cluster are as close to each other as possible, and as far from objects in other clusters as possible. K-means clustering requires that you specify the number of clusters to be partitioned and a distance metric to quantify how close two objects are to each other. Since the color information exists in the ‘a*b*’ space, the objects are pixels with ‘a*’ and ‘b*’ values. K-means clusters the objects into three clusters using the Euclidean distance metric. For every object in the input image, K-means returns an index corresponding to a cluster (see Figure 1). The right most image in Figure 2 is segmented into Regions of Interest.

2.1.2. Identification of individual objects

The identification of objects within an image can be a very difficult task. One way to simplify the problem is to change the grayscale image into a binary image, and morphological operations are then used on these binary images. This phase identifies individual object (cigarette) boundaries and marks the centre of each object for further processing.

Step1: Create a improved binary image by thresholding and morphological operations

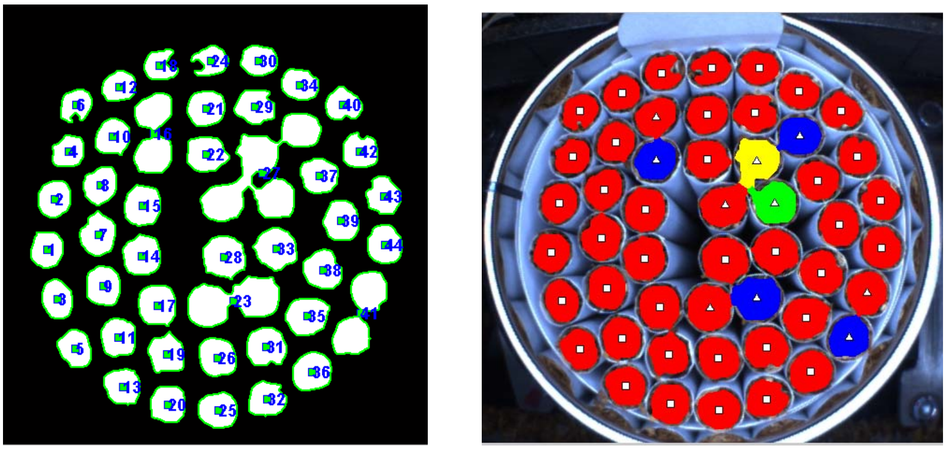

Figure 4. Object Boundary and Centroid estimation

[Left Image] Labelled Image: green lines show the boundary of each object, green squares represent the centre of each object, and the objects are labelled by the blue numbers.
[Right Image] Red regions represent the initial segmented regions. Blue, yellow and green regions are newly divided regions from the first segmented region. The white squares represent the centre of the objects and the white triangles represent the new centres of the re-clustered objects.

First, we produce a binary image from the segmented RGB images. Thresholding is used to convert the segmented image to a binary image. The output binary image has values of 1 (white areas in the left image of Figure 3.) for all pixels and 0 (black) for all other pixels. However the segmentation suffers from inaccuracy because paper-like colours exist in the cigarette and they are segmented as parts of background.

The other obstacle to identification of individual objects is due to contact between objects. These connection inaccuracies should be reduced before further processing. We use morphological operations to reduce them by improving the binary images. Morphological operations are methods for processing binary images based on shapes. As binary images frequently result from segmentation processes on grey level images, the morphological processing of the binary result permits the improvement of the segmentation result. These improved images therefore increase the accuracy of object identification. The morphological operation is performed in two steps: (i) The *shrink* operation is used to remove pixels so that objects without holes shrink to a point, and objects with holes shrink to a connected ring halfway between each hole and the outer boundary. (ii) To fill a small hole, we set a pixel to 1 if five or more pixels in its 3-by-3 neighbourhood are 1's; otherwise, we set the pixel to 0.

Step2: Label the binary image

Contiguous regions are labeled to be identified as an individual object. The k^{th} region includes all elements in the labeled image L that have value k. For example, the pixels labeled 1 make up one object, the pixels labeled 2 make up a second object, and so on. Therefore, the number of objects in L is equal to max(L).

Step3: Separate the joined objects

Table 2 .The examples of the good cases and the defective cases

GOOD CASES	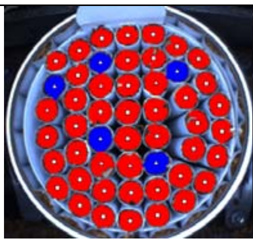	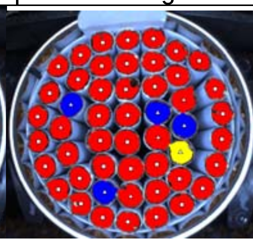	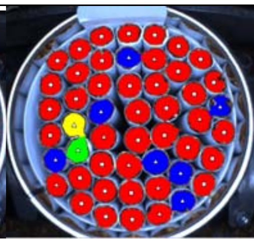	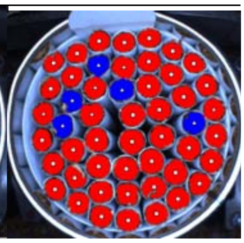
DEFECTIVE CASES		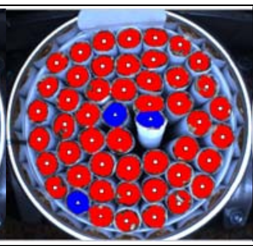	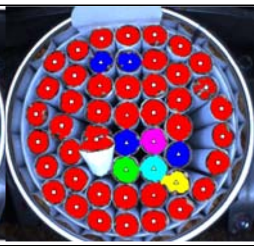	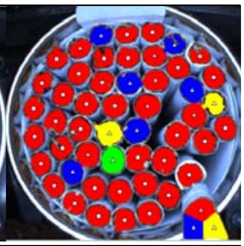

In figure 4 (left image), the identified objects labeled object 16, 23 and 41, contains two physical objects and the identified object labeled 27 contains four physical objects. Therefore, the joined objects should be separated to be an individual object. We use K-mean classification to separate them. The average number of pixels in one cigarette image is 1800 pixels, therefore, to obtain how many individual cigarette in the labeled object, K is calculated by (Area/unit_pixels) + 1, where *Area* is the area of the labeled object and *unit_pixels* is 1800. If K is greater than 1, the object is re-clustered into K clusters (see Figure 4).

The final image includes only the cigarette objects, and the number of objects in the image and the centre points of each object are obtained from this final image. This information is very useful for the classification of defective cases.

2.2. Paper "spoon" handle identification

A paper handle, called a "spoon", is used to pull out the cigarettes from the tin container. It is made of paper and forms part of the packaging inside the cigarette tin. It is located on the circumference of the cigarette package and when viewed from above in an image, it appears as a semicircular object (see Figure 6-d). If the spoon is missing then the cigarette package should be defected. It is therefore important to also recognize from an image the presence of a complete paper spoon component in the package.

Normally the spoon is on the cigarette package circumference on the extreme right of the image. However, due to movement in the manufacturing process, while it will always be on the circumference of the cigarette package, it may be displaced slightly in the image.

If the location of the spoon is always the same in images, then simply applying a semi-circular template of the spoon as a window will identify its presence. However, when the locations of the spoons vary around the circumference, say with a variation of (± α) degrees from the extreme right of the image, then the simple template method is not sufficient. Therefore, we need to develop a new method to detect images that do not display a correct paper spoon so they can be classified as defective packages. This method is explained below:

(a) Grayscale image, I (b) threshold: I = 1 (c) Simplify image (d) Hough transform (e) Convert to BW (f) Set a mask, MI

Figure 5. Create a mask

(a) Grayscale image, I (b) threshold, level 0.9 (c) Fill the image, FI (d) FI – MI, paper spoon

Figure 6. Segment a paper spoon

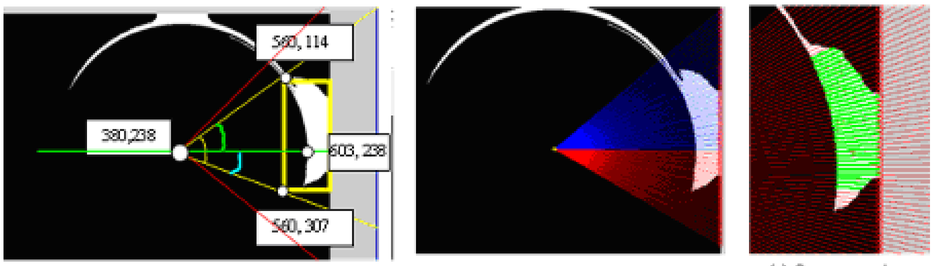

(a) Estimation of the range of radar beam (b) Blue beam (0° to 40°), red beam (330° to 360°) (c) Green mark: a paper spoon

Figure 7. Create radar beams

Step 1: create a mask image

First, we segment the boundary of a tin by the threshold of the maximum intensity (Figure 5). The Hough transform space of this threshold image is able to indicate the center (c_x, c_y) of a tin. An average distance between the initial tin boundary and the centre is the approximation of a radius of the tin. A circle with this centre and radius is taken as a mask (see Figure 5).

Step 2: segment a paper spoon

We segment a paper spoon from the grayscale image by the threshold (Figure 6). The initial area including paper spoon in the image can be segmented with luminance greater than 0.9. The paper spoon is segmented by masking with the image mask created in Step 1 (see Figure 6).

Step 3: detect a paper spoon

A "radar beam" is set up using the center (c_x, c_y). The radar beam is a linear scan radiating from the estimated center of the mask. The radar beams will only scan from 0° to 40°, and from 330° to 360°, since this range will cover the average location of paper spoons ±α, that is any taking the maximum amount of displacement of the paper spoon handle due to processing movement to be ±30° from its ideal manufactured position. As Figure 7 shows, when the red beam cross the paper spoon image, it obtains the width of the paper spoon handle from the image. If the width is equal to or bigger than 20 pixels, we count this as part of the paper handle and the radar beam line is said to represent a "valid line". If the width is less than 20 pixels then it is rejected as noise and the radar beam is not included in the valid set of lines. If there are more than 20 valid lines, the image has a paper handle.

3. Experimental Results

We tested our method on 400 good cases and 100 defective cases. The defective cases include 11 images without the paper spoons (defective cigarette packages that should be rejected). Our system detected the main defective cases, comprising incorrect numbers of cigarettes and missing paper spoons. Our method correctly detected all defective cases (100(true positives)/ (100(true positives) + 0(false negatives) = 1 (sensitivity)). The specificity is (373 (true negatives) / (373 (true negatives) + 27(false positives) = 0.933). The success of our algorithm is shown by its ability to identify almost all the individual objects in the tins (see Table 3). From the defective cases, our method segmented all objects when the size was reasonable (more than 300 pixels). The success of our algorithm is also seen by its ability to detect all defective cases (Table 3).

Table 3. Results

	Detected as defective cases	Detected as good cases
Defective cases (100)	100 (True positive)	0 (False negative)
Good cases (500)	27 (False positive)	373 (True negative)

4. Conclusions

This paper examined the problem of identifying individual cigarettes, and the paper spoon handle in cigarette packages in tin packing manufacturing process. It proposed new algorithms for the identification of these objects using image processing and morphology operations. The identified objects are used to the defect detective packages in the cigarette packing industries. This paper demonstrated the success of the proposed algorithms in correctly identifying individual cigarettes and the paper spoons handles in 500 images and then classifying the resulting cigarette tins as either acceptable or defective.

References

[1] Hamey, L. G. C. and Priest, C., Automatic number plate recognition for australian conditions, Proceeding of the Digital Image Computing on Techniques and Applications, 2005.

[2] Hamey, L. G. C., Yeh, J. C. H., Westcott, T. and Sung, S. K. Y., Pre-processing colour images with a self-organising map: baking curve identification and bake image segmentation, Proceedings of the Fourteenth International Conference on Pattern Recognition, 2:1771-1775, 1998.

[3] Li, S. and Hou, X., Research on the AGV based robot system used in substation inspection, International Conference on Power System Technology, 2006.

[4] Malcolm, A. A., Leong, H. Y., Spowage, A. C. and Shacklock, A. P., Image segmentation and analysis for porosity measurement, Journal of Materials Processing Technology, 192-193:391-396, 2007.

[5] Mari, M., Dambra, C., Chetverikov, D., Verestoy, J., Jozwik, A., Nieniewski, M., Chmielewski, L., et al., The CRASH project: defect detection and classification in ferrite cores, Image Analyisis and Processing-Special Session on European Projects, 1311/1997:781-787, 1997.

[6] Ng, H.-F., Automatic thresholding for defect detection, Pattern Recognition Letters, 27(14):1644-1649, 2006.

[7] Renovell, M., Azaïs, F. and Bertrand, Y., Improving defect detection in static-voltage testing, IEEE Design & Test, 19(6):83-89, 2002.

[8] Elbehiery, H., Hefnawy, A. and Elewa, M., Surface defects detection for ceramic tiles using image processing and morphological techniques, Proceedings of World Academy of Science, Engineering and Technology, 5:1307-6884, 2005.

[9] Costa, C. E. and Petrou, M., Automatic registration of ceramic tiles for the purpose of fault detection, Machine Vision and Applications, 11:225-230, 2000.

[10] Coulthard, M. A., Image processing for automatic surface defect detection, Third Conference on Image Processing and its Applications:192-196, 1989.

[11] Elbehiery, H. M., Hefnawy, A. A. and Elewa, M. T., Visual inspection for fired ceramic tile's surface defects using wavelet analysis, ICGST International Journal on Graphics, Vision and Image Processing, 5(2), 2005.

[12] López, F., Acebrón, F., Valiente, J. M. and Pérez, E., A study of registration methods for ceramic tile inspection purpose, Proceedings of the IX Spanish Symposium on Pattern Recognition and Image Analysis:145-150, 2001.

[13] Smith, M. L. and Stamp, R. J., Automated inspection of textured ceramic tiles, Computers in Industry, 43:73-82, 2000.

[14] Yeh, J. C. H., Hamey, L. G. C., Westcott, T. and Sung, S. K. Y., Colour bake inspection system using hybrid artificial neural networks, IEEE International Conference of Neural Networks:37-42, 1995.

[15] Segnini, S., Dejmek, P. and Öste, R., A low cost video technique for colour measurement of potato chips, Lebensm-Wiss. U-Technology, 32:216-222, 1999.

[16] Kwak, C., Ventura, J. A. and Tofang-Sazi, K., Automated defect inspection and classification of leather fabric, Intelligent Data Analysis, 5:355-370, 2001.

[17] Abou-Taleb, H. A. and Sallam, A. T. M., On-line fabric defect detection and full control in a circular knitting machine, AUTEX Research Journal, 8:21-29, 2008.

[18] Convery, S., Lunney, T., Hashim, A. and McGinnity, M., Automated fabric inspection, International Journal of Clothing Science and Technology, 6:15-19, 1994.

[19] Perez, R., Silvestre, J. and Munoz, J., Defect detection in repetitive fabric patterns, Proceeding of Visualization, Imaging and Image Processing, 2004.

[20] Tajeripour, F., Kabir, E. and Sheikhi, A., Fabric defect detection using modified local binary patterns, EURASIP Journal on Advances in Signal Processing, 2008, 2008.

[21] Uçar, N. and Ertuğrul, S., Prediction of fuzz fibers on fabric surface by using neural network and regression analysis, Fibres & Textiles in Eastern Europe, 15:58-61, 2007.

[22] Yang, X., Pang, G. and Yung, N., Robust fabric defect detection and classification using multiple adaptive wavelets, IEE proceeding on Image Signal Process, 2005.

[23] Zhi, Y. X., Pang, G. K. H. and Yung, N. H. C., Fabric defect detection using adaptive wavelet, IEEE International Conference on Acoustics, Speech and Signal Processing, 2001.

[24] Mery, D. and Pedreschi, F., Segmentation of colour food images using a robust algorithm, Journal of Food Engineering, 66:353-360, 2005.

[25] Yam, K. L. and Papadakis, S. E., A simple digital imaging method for measuring and analyzing color of food surfaces, Journal of Food Engineering, 61:137-142, 2004.

[26] Abdullah, M. Z., Guan, L. C., Lim, K. C. and Karim, A. A., The applications of computer vision system and tomographic radar imaging for assessing physical properties of food, Journal of Food Engineering, 61:125-135, 2004.

[27] Hatcher, D. W., Symons, S. J. and Manivannan, U., Developments in the use of image analysis for the assessment of oriental noodle appearance and colour, Journal of Food Engineering, 61:109-117, 2004.

[28] Braxakovic, D., Beck, H. and Sufi, N., An approch to defect detection in materials characterized by complex textures, Pattern Recognition, 23(1/2):99-107, 1990.

[29] Kauppinen, H., Rautio, H. and Silvén, O., Non-segmenting defect detection and SOM based classification for surface inspection using color vision, Conference on Polarization and Color Techniques in Industrial Inspection (SPIE 3826):270-280, 1999.

[30] Brosnan, T. and Sun, D., Improving quality inspection of food products by computer vision - a review, Journal of Food Engineering, 61:3-16, 2004.

[31] Du, C.-J. and Sun, D.-W., Recent developments in the applications of image processing techniques for food quality evaluation, Trends in Food Science & Technology, 15:230-249, 2004.

[32] Zhang, Y. F. and Bresee, R. R., Fabric defect detection and classification using image analysis, Textile Research Journal, 65(1):1-9, 1995.

[33] Hunter and Sewall, R., Photoelectric Color-Difference Meter, Proceedings of the Winter Meeting of the Optical Society of America, 38(7):661, 1998.

[34] Hunter and Sewall, R., Accuracy, precision, and stability of new photo-electric color-difference meter, proceedings of the Thirty-Third Annual Meeting of the Optical Society of America, 38(12):1094, 1991.

[35] Forsyth, D. and Ponce, J., Computer vision: a modern approach New Jersey: Pretice Hall, 2003.

[36] Hunt, R. W. G., Measuring colour, 2nd Ellis Horwood, Ltd, 1991.

[37] León, K., Mery, D., Pedreschi, F. and León, J., Color measurement in L*a*b* units from RGB digital images, Food Research International, 39:1084-1091, 2006.

[38] Stöderström, T. and Stoica, P., System identification, New York: Prentice-Hall, 1989.

Authors

Mira Park graduated with a PhD in Computer Science Engineering from the University of New South Wales in 2003. During 2004~2005, she worked as a research fellow in the Computer Science and Software Engineering department at the University of Melbourne. She is a research fellow in the school of Design, Communication and IT at the University of Newcastle. Her research interests are Computer Vision, Pattern Recognition, and Medical Imaging.

Prof. Jesse S. Jin graduated with a PhD from the University of Otago, New Zealand in 1992. He is currently the Chair of IT in the University of Newcastle. He also chairs the Academic Board at the College of Arts and Commerce, Raffles University. He has published 250 articles and 11 books, and filed three patents. He established a spin-off company and the company won the 1999 ATP Vice-Chancellor New Business Creation Award. He is a consultant of many companies such as Motorola, Computer Associates, ScanWorld, Proteome Systems, Hyper Soft, etc. His research interests include Medical Imaging, Multimedia, Computer Vision and Pattern Recognition.

Suhuai Luo received the B.E. and M.E. degrees in Radio Engineering from Nanjing University of Posts and Telecommunications China in 1982 and 1987, respectively, and PhD degree in Electrical Engineering from the University of Sydney Australia in 1995. From 1995 to 2004, he worked as a senior research scientist with the Commonwealth Scientific and Industrial Research Organization Australia and the Bioinformatics Institute Singapore. He is now a senior lecturer with the University of Newcastle Australia. His research interests include biomedical signal processing, image and video processing, computer vision, and internet-oriented IT applications.

Yue Cui received the B.E. and M.E. degrees in Computer Science and Technology from Jilin University of China in 2004 and 2007 respectively. She is a PhD student in The University of Newcastle Australia. Her research interests include Image Processing and Computer Vision.